

1 **Internal tree cycling and atmospheric archiving of mercury: examination with
2 concentration and stable isotope analyses.**

3 *David S. McLagan^{1,2,3}, Harald Biester¹, Tomas Navrátil⁴, Stephan M. Kraemer⁵, Lorenz Schwab^{5,6}*

4 ¹Institute of Geoecology, Technical University of Braunschweig, Braunschweig, 38106, Germany

5 ²Dept. of Physical and Environmental Sciences, University of Toronto Scarborough, M1C1A4 Canada

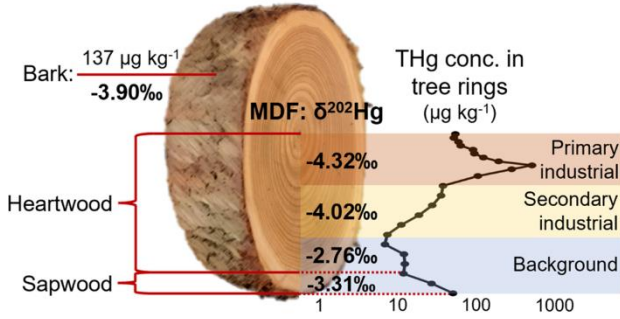
6 ³School of Environmental Studies and Dept. of Geological Sciences and Geological Engineering, Queen's
7 University, K7L3N6 Canada

8 ⁴Institute of Geology of the Czech Academy of Sciences, Prague, 117 20, Czech Republic

9 ⁵Department for Environmental Geochemistry, Centre for Microbiology and Environmental Systems
10 Science, University of Vienna, Vienna, 1090, Austria

11 ⁶Doctoral School in Microbiology and Environmental Science, University of Vienna, Vienna, 1090, Austria

12 *Correspondence to: david.mclagan@queensu.ca*



14 **Abstract.** Trees predominantly take up mercury (Hg) from the atmosphere via stomatal assimilation of
15 gaseous elemental Hg (GEM). Hg is oxidised in leaves/needles and transported to other tree anatomy
16 including bole wood where it can be stored long-term. Using Hg associated with growth rings facilitates
17 archiving of historical GEM concentrations. Nonetheless, there are significant knowledge gaps on the
18 cycling of Hg within trees. We investigate Hg archived in tree rings, internal tree Hg cycling, and differences
19 in Hg uptake mechanisms in Norway spruce and European larch sampled within 1 km of a HgCl_2
20 contaminated site using total Hg (THg) and Hg stable isotope analyses. Tree ring samples are indicative of
21 significant increases in THg concentrations (up to $521\mu\text{g kg}^{-1}$) from *background period* (BGP; facility
22 closed; 1992—present) to *secondary industrial period* (2ndIP; no HgCl_2 wood treatment; 1962–1992) to
23 *primary industrial period* (1stIP; active HgCl_2 wood treatment; \approx 1900–1962). Mass dependent fractionation
24 (MDF) Hg stable isotope data are shifted negative during industrial periods ($\delta^{202}\text{Hg}$: 1stIP: $-4.32 \pm 0.15\text{‰}$;
25 2ndIP: $-4.04 \pm 0.32\text{‰}$; BGP: $-2.83 \pm 0.74\text{‰}$; 1SD). Even accounting for a \approx -2.6‰ MDF shift associated with
26 stomatal uptake, these data are indicative of emissions derived from industrial activity being enriched in
27 lighter isotopes associated with HgCl_2 reduction and Hg^0 volatilisation. Similar MDF ($\delta^{202}\text{Hg}$: $-3.90 \pm$
28 0.30‰ ; 1SD) in bark Hg ($137 \pm 105\mu\text{g kg}^{-1}$) suggests that stomatal assimilation and downward transport is
29 also the dominant uptake mechanism for bark Hg (reflective of negative stomatal uptake MDF shift) rather
30 than deposition to bark. THg was enriched in sapwood of all sampled trees across both tree species. This
31 may indicate long-term storage of a fraction of Hg in sapwood or xylem solution. We also observed a small
32 range of odd isotope-MIF. Differences in $\Delta^{199}\text{Hg}$ between periods of different industrial activities were

33 significant ($\Delta^{199}\text{Hg}$: 1stIP: $0.00 \pm 0.03 \text{‰}$; 2ndIP: $-0.06 \pm 0.04 \text{‰}$, BGP: $-0.13 \pm 0.03 \text{‰}$, 1SD), and we
34 suggest MIF signatures are conserved during stomatal assimilation (reflect source MIF signatures). These
35 data advance our understanding of the physiological processing of Hg within trees and provide critical
36 direction to future research into the use of trees as archives for historical atmospheric Hg.

37 Key words

38 Mercury biogeochemistry, tree rings, sapwood (hydroactive xylem), heartwood, phloem, bark, process and
39 source tracing.

40 1. Introduction

41 Until the last 10—15 years, it was hypothesised that the major transfer pathway of mercury (Hg) from the
42 atmospheric to terrestrial and aquatic matrices was the wet and dry deposition of Hg(II) as either gaseous
43 oxidised Hg (GOM) or particulate bound-Hg (PBM) (Lin and Pehkonen, 1999; Lindberg et al., 2007; Selin,
44 2009). However, studies began to suggest that dry deposition of gaseous elemental Hg (GEM) had to be
45 more important than was thought because of inconsistencies between measurement data of atmospheric Hg
46 species and modelling predictions (Selin et al., 2008; Zhang et al., 2009; Mao and Talbot, 2009). A major
47 mechanism for dry deposition of GEM is uptake and assimilation to flora via stomata during plant
48 respiration, an idea that was posited by scientists as far back as the late 1970s (Browne and Fang, 1978;
49 Lindberg et al., 1979). The rate of GEM uptake correlates to photosynthetic activity of the plants (Laacouri
50 et al., 2013), but is also species dependent since it is related to stomatal conductance and the number of
51 stomata per leaf (Millhollen et al., 2006; Laacouri et al., 2013). Recent work has provided evidence that dry
52 deposition of GEM to vegetation via stomatal uptake and subsequent transfer via leaf/needle senescence,
53 abscission, and litterfall is likely to be the dominant mechanism for Hg deposition from the atmosphere to
54 terrestrial matrices (Obrist et al., 2017; 2018; Jiskra et al., 2018). Similarly, there is strong evidence that
55 GEM is also the major source of Hg in bole wood of trees (Scanlon et al., 2020, Wang et al., 2020; 2021).
56 Using Hg stable isotope measurements, stomatal assimilation of GEM deposition has been estimated to
57 supply 57—94 % of total Hg (THg) in vegetated terrestrial systems (Khan et al., 2019 and references
58 therein). A major loss mechanism of Hg from forest ecosystems is during biomass burning (Friedli et al.,
59 2009; McLagan et al., 2021a; Dastoor et al., 2022).

60 To assess Hg cycling within trees we must also reflect on alternative uptake mechanisms: (i) uptake from
61 roots and (ii) deposition to above ground tree surfaces (stems, leaves, and bark) and potential sorption to and
62 translocation into tree tissue. Hg uptake from roots has been studied for decades. Data overwhelmingly show
63 minimal transport of Hg from the root zone to aerial mass of trees (Beauford et al., 1977; Lindberg et al.,
64 1979; Bishop et al., 1998; Moreno et al., 2005; Graydon et al. 2009; Cui et al., 2014; Cozzolino et al., 2016;
65 Peckham et al., 2019a). Even in soils with elevated THg concentrations, upward transfer from roots is low in
66 relative terms (Beauford et al., 1977; Lindberg et al., 1979; Graydon et al. 2009). Limited uptake of Hg and
67 other metals via the roots has been attributed to restrictive barriers in the roots such as that provided by the
68 endodermis (Kahle, 1993). Alternatively, Hg can also be deposited to surfaces of the aerial anatomy of trees,
69 predominantly as GOM and PBM (Rea et al., 2002; Mowat et al., 2011; Laacouri et al., 2013). Hg on leaf
70 surfaces contributes only a minor fraction of THg in foliage and accumulation rates are low due to both
71 precipitation wash-off (Rea et al., 2000; 2001; Laccouri et al., 2013) and photoreduction and subsequent
72 evasion of GEM (Graydon et al., 2006; Mowat et al., 2011). Several studies have demonstrated elevated bark
73 THg concentrations relative to branch and bole wood (Siwik et al., 2010; Zhou et al., 2017; Liu et al., 2020).
74 Therefore, it has been suggested that Hg in bark is chiefly derived from atmospheric deposition (Chiarantini
75 et al., 2016; 2017) potentially with a greater proportion of GOM and PBM rather than GEM (Peckham et al.,
76 2019a).

77 Trees make up a large sink for atmospheric Hg and therefore play an important role in the global Hg cycle.
78 Hg has no known biological function in plants (Moreno-Jiménez et al., 2006; Peralta-Videa et al., 2009;
79 Cozzolino et al., 2016); thus, it is important to understand the physiological processing of Hg within trees
80 from a phytotoxicological standpoint. After assimilation through leaf/needle stoma GEM is assumed to be
81 oxidised to form Hg(II) compounds and integrate with internal leaf tissue (Laacouri et a., 2013; Demers et
82 al., 2013). A recent study examining three evergreen species used Hg stable isotopes to show that reduction
83 and re-release can occur (Yuan et al., 2018). Although the bole wood of trees has lower THg concentrations
84 than bark and needles/leaves in both deciduous and evergreen species (Navrátil et al., 2017; Zhou et al.,
85 2017; Liu et al., 2020), the overall Hg loading of the tree is the reverse: wood carries the largest total mass
86 of Hg due to much greater overall biomass (Liu et al., 2020).

87 Hg is transported from the foliage to bole wood via the phloem, which is the conduit for nutrient and
88 photosynthetic product transfer from leaves/needles to the rest of the trees (Cutter and Guyette, 1993).
89 Phloem ([first layer of inner bark](#)) lies between the cambium (tissue that promotes new xylem and phloem
90 growth) and the [inner bark](#)[cork](#) and [outer bark](#). Once oxidised to Hg(II) species in the leaves/needles, it likely
91 associates with phytochelatin, cysteine compounds for phloem transport (O'Connor et al., 2019; Dennis et
92 al., 2019). Phloem-to-xylem translocation (new xylem makes up sapwood and forms tree rings) is expected
93 to occur throughout this downward transport (Arnold et al., 2018; Yanai et al., 2020; Nováková et al., 2021;
94 2022). This translocation likely proceeds via *rays*, parenchyma cells that radially connect xylem and phloem
95 conductive tissues and mediate water and nutrient transport, tree growth, and biotic and abiotic stressors
96 (Nagy et al., 2014; Pfautsch et al., 2015; Gustin et al., 2022). THg is expected to be preserved in the newly
97 forming xylem tree rings; and hence, THg concentrations in tree rings have been used as a proxy for
98 historical atmospheric GEM concentration (Siwik et al., 2010; Wright et al., 2014; Clackett et al., 2018).
99 This includes identification of elevated GEM concentrations, past and present, associated with atmospheric
100 Hg emissions from industrial activities located near sampled trees (Odabasi et al., 2016; Navrátil et al., 2017;
101 Scanlon et al., 2020; Nováková et al., 2022). A potential caveat to this method of chronicling historical
102 atmospheric GEM concentrations is the translocation of Hg between tree rings that has been reported in
103 certain studies; tree ring concentrations do not reflect reported industrial activity (Nováková et al., 2021;
104 Wang et al., 2021). However, there are a number of studies that demonstrate this inter-ring translocation does
105 not significantly influence results; tree ring Hg concentrations reflect reported industrial (Clackett et al.,
106 2018; Navrátil et al., 2018; Peckham et al., 2019b). Tree species may be a factor affecting inter-ring Hg
107 translocation (Scanlon et al., 2020; Nováková et al., 2021).

108 Hg stable isotopes represent a powerful and relatively new technique that can provide information relating to
109 the biogeochemical cycling history and potentially source information of sampled Hg (Bergquist and Bloom
110 2007; 2009). This premise assumes distinct “signature” ratios of different sources, and mass-dependant
111 (MDF) and mass-independent (MIF) fractionations of the seven stable Hg isotopes that can be imparted by
112 environmental transformation processes (Bergquist and Bloom 2007; 2009). Forest ecosystems are no
113 exception to this. For instance, Hg stable isotopes added substantial evidence to the argument that GEM
114 stomatal assimilation and eventual litterfall (or vegetation death) was the dominant mechanism for Hg
115 deposition to soils in vegetated ecosystems (Wang et al., 2017; Jiskra et al., 2018; Yuan et al., 2018). Studies
116 examining Hg stable isotopes in tree-rings are limited (Scanlon et al., 2020; Wang et al., 2021). Both studies
117 associated differences in MIF ($\Delta^{199}\text{Hg}$) with varying sources over time, but Wang et al. (2021) suggested
118 there were limitations to this interpretation due to inter-ring translocation of Hg. They also attribute
119 differences in MDF ($\delta^{202}\text{Hg}$) with physiological differences (i.e., inter-ring translocation, stomatal
120 conductance, and canopy dynamics), particularly as they relate to tree species, and environmental factors
121 (i.e., soil conditions, slope, and winds) (Wang et al., 2021).

122 In this study, we examine THg concentrations and stable isotopes in two coniferous tree species, Norway
123 spruce (*Picea abies*) and European larch (*Larix decidua*), surrounding a legacy Hg contaminated site in the
124 German Black Forest. We aim to investigate if historical records of the industrial activities correlate with
125 elevated THg concentrations in tree rings of sampled trees. There are no records of historical atmospheric Hg
126 emissions or concentrations at this site, which was subject primarily to soil and water contamination
127 (application of low-volatility HgCl₂ solution) rather than combustion emissions to the atmosphere. Thus, we
128 compliment tree-ring data with deployments of GEM passive air samplers (PASs) at the site to assess
129 atmospheric GEM conditions at the former industrial site past (tree rings) and present (PASs). Using Hg
130 stable isotopes, we aim to examine potential source related variations in MDF and MIF across the tree ring
131 records and physiological processes that may separate pools of Hg in the transport mechanism from
132 atmosphere to foliage to phloem to tree-ring/bole wood. Additionally, we aim to investigate if deposition and
133 sorption of Hg to tree bark is the dominant mechanism for bark Hg (isotopically distinct from bole wood).

134 **2. Methods**

135 **2.1. Study site**

136 The study area is in the High Black Forest (\approx 850 m a.s.l.) in Baden-Württemberg, Germany. Trees were
137 sampled within a 1 km radius of a former kyanisation facility that treated timber with \approx 0.66% HgCl₂ solution
138 for preservation with substantial losses of this contaminated solution to soils, groundwater, and stream water
139 (Eisele, 2004, Richard et al., 2016; McLagan et al., 2022). Although the trees were sampled within a 1 km
140 radius of the contaminated site, all trees were outside, and upslope of the area directly affected by Hg
141 contamination to soils and groundwater. The location of the sampled trees, former industrial buildings, wood
142 drying areas, and passive sampling locations are shown in Fig. 1. The history of the industrial activities at the
143 site can be divided into three distinct periods:

- 144 1. *Primary (first) industrial period (1stIP; 1892-1961):* Reports on this contaminated site describe the
145 operation of the kyanisation facilities (wood treatment with 0.66 % HgCl₂) from 1892 until site
146 owners went bankrupt in 1961 (Weis, 2020; Eisele, 2004; Schrenk and Hiester, 2007).
- 147 2. *Secondary industrial period (2ndIP; 1962-1992):* The site was acquired by another company and
148 wood use and timber production as well as storage of timber treated with HgCl₂ is reported to have
149 continued at the site until 1992 (Eisele, 2004; Schrenk and Hiester, 2007).
- 150 3. *Background period (BGP; 1992-present):* The site lay fallow between 1992 and 2002 before site
151 remediation (2002—2004) and conversion of the area to a commercial space (Eisele, 2004; Schrenk
152 and Hiester, 2007).

153 These three periods will be referred to throughout the study under the descriptors of 1stIP, 2ndIP, and BGP,
154 respectively.

155 **2.2. Sampling and sample preparation**

156 Bole wood (tree ring) samples were collected via two methods. The first was using a 450 mm long, 5.15 mm
157 diameter increment borer (Haglöf Sweden). The tree core was sampled at breast height (\approx 1.2—1.5 m above
158 ground). Whole tree core samples were placed in lab grade sampling straws and double zip-seal bags for
159 transport back to the lab, immediately frozen at -20 °C upon return, subsequently freeze dried (-80 °C and 7
160 pa), and then stored at room temperature in conical centrifuge tubes until analysis. Spruce 1—3, Spruce BG,
161 and Larch 1—3 were all sampled by this method. Samples processed by this method were counted for rings,
162 cut with a lab scalpel, and weighed into nickel boats for analysis after being freeze-dried. Samples were
163 counted for the visibly defined rings and cut with a disposable scalpel.

164 The second method involved the collection of freshly cut (collected on day of tree felling) tree slices or
165 “cookies” (see TOC art; Section S1) from \approx 0.5 m above the ground. A \approx 50 mm slice was cut from the
166 middle of each tree cookie with a large table saw. Individual Tree ring samples of aggregated tree rings
167 were cut from this slice with a plain edge chisel and All exposed sides we cut away and discarded.
168 Samples were then frozen and freeze dried, and then stored at room temperature in conical centrifuge tubes
169 until analysis. Spruce ISO4—6 were sampled by this method.

170 The number of tree rings (temporal resolution) in any given sample was typically 5 years but varied
171 somewhat with higher resolution in samples from some trees during 1stIP and 2ndIP, and lower in some
172 samples from Spruce ISO trees that required higher THg concentrations per sample for Hg stable isotope
173 analyses. Samples were counted for rings, cut with a lab scalpel, weighed into nickel boats and then
174 combusted at 750 °C for 300 seconds. Care was taken to remove bark and phloem from wood, but there may
175 have been instances where some phloem remained attached to the newest tree ring sample. Bark was
176 sampled from Spruce ISO4—6. Bark from Spruce ISO4 and Spruce ISO5 were divided into inner and outer
177 bark (estimated as the middle of the bark) using a disposable scalpel. These bark samples were then frozen
178 and freeze dried, and then stored at room temperature in conical centrifuge tubes until analysis. After sample
179 preparation samples were frozen (–20 °C), then freeze dried (–80 °C and 7 pa), and subsequently stored at
180 room temperature until analysis. Cleaning methods for equipment and surfaces is detailed in Section S1. As
181 these samples are from living (or freshly cut) trees and not sampled on an annual temporal resolution (there
182 were multiple tree rings in each sample) no cross dating methods were necessary; ring counting represents
183 the most accurate method of dating. Sapwood was visually identified by colour changes (Bertaud and
184 Holmbom, 2004). However, any uncertainty associated with identification of the exact number of sapwood
185 rings is of little consequence to the study as the greatest THg enrichment in sapwood was in the youngest
186 tree rings, which, we can state with certainty, were sapwood rings.

187 2.3. Total Hg analyses

188 THg concentration of samples collected with the increment borer were made using a thermal desorption,
189 amalgamation and atomic adsorption spectrometry (DMA80, Milestone Instruments). Samples were counted
190 for rings, cut with a lab scalpel (see borer cleaning methods), weighed into nickel boats and then combusted
191 at 750 °C for 300 seconds. Reference materials, Apple leaves (SRM 1515, NIST) and China Soil (NCS-
192 DC73030; China National Analysis Centre for Iron and Steel), were measured throughout the analyses and
193 the recoveries were $103 \pm 3\%$ ($n = 30$) and $99 \pm 5\%$ ($n = 11$), respectively. Details of the GEM passive air
194 sampler methods and data can be found in Section S2. THg concentration for the ISO trees were calculated
195 from the analysis of traps after the pre-concentration for isotope analysis (DMA-80L). All samples were
196 considered on a dry-weight basis (after freeze-drying) to remove any potential bias associated with moisture
197 loss during transport and storage before freezing.

198 2.4. Hg stable isotope analyses

199 Hg stable isotope analyses were performed on tree slice samples from trees: Spruce ISO4—6. No larch trees
200 could be analysed for Hg stable isotopes as no larch tree slices could be collected. The low THg
201 concentration in many sections of the wood is a challenge for Hg stable isotope analyses. Low concentration
202 samples required pre-concentration and trapping by combusting samples in a DMA80 and then purging the
203 released Hg from multiple boats of the same sample into 5 mL traps consisting of 40 % (v/v) inverse aqua
204 regia that replaced HCl with BrCl. Further method details and quality control/assurance of these analyses are
205 provided in Section S4 (see also McLagan et al. (2022)). Traps with insufficient concentrations for isotope
206 analysis were pool using the purge and trap method detailed in Section S5. Hg stable isotope measurements
207 were made using a Nu Plasma II (Nu Instruments) inductively coupled plasma mass spectrometer (MC-ICP-
208 MS) connected to an HGX-200 cold vapour generator for Hg introduction (Teledyne Cetac) and a

209 desolvating nebulizer for external mass bias correction by Tl doping using NIST-997 (Aridus 2, Teledyne
210 Cetac) following a method previously established in our laboratory (see McLagan et al. (2022) and
211 Wiederhold et al. (2010) for method details). All samples and standards were diluted to match concentrations
212 within each session and samples were measured using standard bracketing with NIST-3133. Analytical
213 precision (2SD) and accuracy (using repeated measurements of “in-house” *ETH Fluka* standard ~~and NIST~~
214 ~~3133~~ standards) for these analyses are reported in Section S6 along with full Hg stable isotope datasets.
215 Isotope ratios are reported as the deviation from the isotopic composition of the NIST-3133 standard using
216 delta notation and expressed in per mil (‰) (details in Section S4).

217 **3. Results and Discussion**

218 **3.1. Elevated tree ring total Hg concentrations during industrial activity**

219 Elevated THg concentrations were observed in both Norway Spruce (*P. abies*) and European larch (*L.*
220 *decidua*) tree rings dated before the mid-1990s compared to tree rings from the background Norway spruce
221 (Spruce BG), which was situated ≈5.5km west (upwind based on dominant westerly winds in the area) of the
222 former industrial facility (Fig. 2; THg data in Section S4). These species were chosen due to suggested
223 suitability for Hg archiving in previous studies (Hojdová et al., 2011; Nováková et al., 2021) and there was a
224 distinct pattern in tree ring THg concentrations in across all sampled trees near the legacy contaminated site
225 regardless of species. This resulted in four distinct periods: (i) slightly elevated THg concentration in
226 sapwood (hydroactive xylem) rings (0—5, 0—10, or 0—15 year tree rings; see Section 3.3.2 for discussion),
227 (ii) low THg concentration in rings from the *BGP* not influenced by any known industrial activity (1992—
228 sapwood), (iii) increasing THg concentrations in rings from what we term the *2ndIP* (1962—1992), and (iv)
229 very elevated THg concentrations during the active kyanising or *1stIP* (before 1962) (Fig. 2). Not all sampled
230 trees were of sufficient age to cover all of these periods (no larch trees reached the *1stIP*), but all trees that
231 were old enough did follow this trend albeit with some distinct inter-tree differences in THg concentrations
232 (Fig. 2).

233 The THg concentrations ranged from ≈1—10 µg·kg⁻¹ ~~from in heartwood~~ tree rings ~~from in~~ the *BGP*, ~~and~~ up
234 to 521 µg·kg⁻¹ in a sample dated from 1951—1953 during the *1stIP* in Spruce 1, which is ≈400—500 m
235 northeast of the former kyanisation building and wood drying areas. Additionally, THg concentrations of up
236 to 211 µg·kg⁻¹ were measured in a sample dated 1974—1976 (*2ndIP*) in Spruce 2, which was the closest tree
237 sampled to the former facility (≈200—300 m south). However, this tree was planted after the *1stIP*. Distance
238 of the tree from the industrial source was a definite factor in the between tree variability in THg
239 concentrations, which has also been documented by Navrátil et al. (2017) and Nováková et al. (2022). These
240 THg concentrations are comparable to other studies with the high THg concentrations measured in tree rings
241 such as Becnel et al. (2004) (Loblolly Pine and Red Maple; THg concentrations up to 644 µg·kg⁻¹), Abreu et
242 al. (2008) (Black Poplar; THg concentrations up to 280 µg·kg⁻¹), and Nováková et al. (2022) (European
243 larch; THg concentrations up to 249 µg·kg⁻¹). However, the THg concentrations in our study are lower than
244 the very high concentrations measured by Wang et al. (2021) (Masson Pine; THg concentrations up to 2140
245 µg·kg⁻¹), which is likely associated with the source being a former Hg mine known to have emitted large
246 quantities of elemental Hg (Hg(0)) to the atmosphere.

247 The THg concentrations in the tree rings generally provide a good representation of the industrial history of
248 the site based on the applied ≈5-year sampling resolution. While the end of the *2ndIP* falls in the middle of
249 the 25—30 year tree ring samples, there is an increase in THg concentrations in all trees in samples 30—35
250 year and greater (before 1990). This is most apparent in the Spruce 1 and Spruce 2, which are the two
251 sampled spruce trees closest to the former kyanisation building and wood drying sites. The average THg
252 concentration for Spruce 1 and Spruce 2 was significantly higher ($p = 0.031$ and $p < 0.001$, respectively)
253 during the *2ndIP* (1962—1990; Spruce 1: $23.1 \pm 12.8 \mu\text{g}\cdot\text{kg}^{-1}$; and Spruce 2: $134 \pm 56 \mu\text{g}\cdot\text{kg}^{-1}$) than during

254 the *BGP* (1990—sapwood; Spruce 1: $10.8 \pm 2.6 \mu\text{g}\cdot\text{kg}^{-1}$; and Spruce 2: $9.46 \pm 3.65 \mu\text{g}\cdot\text{kg}^{-1}$). There was a
255 sharp increase in THg concentration in the closest larch tree to the site (Larch 1) at this time, but the tree
256 only dated to 1978, which is less than halfway through the *2ndIP*. Spruce 1 was also indicative of
257 significantly higher ($p = 0.007$) THg concentrations during the *1stIP* ($150 \pm 141 \mu\text{g}\cdot\text{kg}^{-1}$) compared to the
258 elevated THg concentrations of the *2ndIP*. These agrees with other studies that have demonstrated good
259 correlations between industrial activity and tree ring Hg (Clackett et al., 2018; Navrátil et al., 2017; 2018;
260 Nováková et al. 2022). Nonetheless, several studies have suggested that Hg can translocate across tree rings,
261 which results in temporal differences between tree ring Hg and reported industrial activities/inventories
262 (Nováková et al., 2021; Wang et al., 2021). This should continue to be monitored closely in future studies,
263 particularly considering the sapwood enrichment discussed in Section 3.3.2.

264 Although the exact location of the three Spruce ISO trees (tree slices collected for Hg stable isotope analysis)
265 is unknown, they were from a deforested stand of spruce between 200—500 m further from the wood drying
266 site than Spruce 1 on an easterly facing slope (away from the site). Consequently, the mean THg
267 concentrations in the Spruce ISO4—6 were generally lower than in Spruce 1. Nonetheless, the same trends
268 were observable: mean THg concentrations during the active industrial period (before 1962, THg: $44.2 \pm$
269 $15.5 \mu\text{g}\cdot\text{kg}^{-1}$) were significantly greater ($p = 0.006$) than during the *2ndIP* (1962—1990, THg: 26.7 ± 15.7
270 $\mu\text{g}\cdot\text{kg}^{-1}$), which were significantly greater ($p = 0.001$) than rings from 1990—sapwood (THg: 6.5 ± 4.6
271 $\mu\text{g}\cdot\text{kg}^{-1}$) based on combined data from all three Spruce ISO trees.

272 **3.2. Isotopically fractionated Hg in tree rings associated with industrial 273 emissions**

274 **3.2.1. Mass dependant fractionation (MDF)**

275 The THg concentration data from tree rings suggest substantial emissions of Hg to the atmosphere during the
276 industrial period. However, the original Hg contamination at these sites was the treatment of timber with
277 HgCl_2 solution, a species that has a high solubility and low volatility compared to $\text{Hg}(0)$ (Henry's Law
278 constant: $\text{Hg}(0)$: $1.4 \times 10^{-3} \text{ mol}\cdot\text{m}^{-3}\cdot\text{Pa}^{-1}$; HgCl_2 : $2.7 \times 10^4 \text{ mol}\cdot\text{m}^{-3}\cdot\text{Pa}^{-1}$; Schroeder and Munthe, 1998). Thus,
279 the majority of any Hg releases to the atmosphere must have occurred via reduction of $\text{Hg}(\text{II})$ to $\text{Hg}(0)$ and
280 subsequent volatilisation as GEM. Kinetic processes such as reduction and evaporation result in the product
281 (Hg released to the atmosphere in this case) becoming enriched in lighter isotopes (more negative $\delta^{202}\text{Hg}$;
282 Bergquist and Blum, 2007; 2009). Like the THg concentrations, MDF values reflect a chronological trend:
283 $\delta^{202}\text{Hg}$ values from the *1stIP* ($\delta^{202}\text{Hg}$: $-4.32 \pm 0.15 \text{ ‰}$, 1SD) were significantly more negative ($p = 0.007$)
284 than during the *2ndIP* ($\delta^{202}\text{Hg}$: $-4.02 \pm 0.31 \text{ ‰}$; 1SD), which in turn were significantly more negative ($p <$
285 0.001) than rings from the *BGP* ($\delta^{202}\text{Hg}$: $-2.76 \pm 0.76 \text{ ‰}$, 1SD; sapwood 0—5 year samples not included, see
286 Section 3.3.2) based on combined data from all three Spruce ISO trees (Fig. 3A). Wang et al. (2021)
287 observed similar, although weaker, trends in Masson pines near Hg contaminated sites in China (range:
288 -5.06 ‰ to -2.53 ‰ ; median: -3.74 ‰). MDF ($\delta^{202}\text{Hg}$) has also been examined in oak ($-1.82 \pm 0.09 \text{ ‰}$) and
289 pitch pine ($-2.98 \pm 0.76 \text{ ‰}$; North America; Scanlon et al., 2020), conifers ($-2.76 \pm 0.46 \text{ ‰}$; China; Liu et al.,
290 2021), evergreen trees ($-3.15 \pm 0.22 \text{ ‰}$; China; Wang et al., 2020), and harvested one-year old Norway
291 spruce saplings ($-2.71 \pm 0.27 \text{ ‰}$; Germany; Yamakawa et al., 2021). $\delta^{202}\text{Hg}$ values in these studies were
292 more similar to samples from the *BGP* in our study, which likely relates to their low bole wood THg
293 concentrations associated with the remoteness of their study sites from contamination sources (Scanlon et al.,
294 2020; Wang et al., 2020; Liu et al., 2021; Yamakawa et al., 2021).

295 McLagan et al. (2022) highlight the difficulties in characterising a specific source signature of Hg stocks
296 used in industrial activities due to the variability in stock $\delta^{202}\text{Hg}$ values, potential change in Hg supplies
297 during the facility's lifetime, and the possibility that the industrial use of Hg resulted in the Hg emitted to
298 different environmental media being fractionated from the original Hg stock. The highly negative $\delta^{202}\text{Hg}$

299 values during both the 1^{st} IP and 2^{nd} IP support the hypothesis that there was significant loss of Hg to the
300 atmosphere during the industrial activities, which would result in the residual HgCl_2 in solution (major
301 source of soil-groundwater contamination) being isotopically heavier than the original Hg stocks used at the
302 site. Indeed, solid phase materials (listed as “SCA1” and “TSA” in McLagan et al., 2022) beneath the former
303 kyanisation plant with THg concentrations $>50 \mu\text{g}\cdot\text{kg}^{-1}$ had mean $\delta^{202}\text{Hg}$ values of $0.06 \pm 0.23 \text{‰}$ (McLagan
304 et al., 2022). This is at the positive end of the range of $\delta^{202}\text{Hg}$ values reported for cinnabar ores and
305 commercial liquid Hg^0 stocks (Sun et al., 2016; Grigg et al., 2018).

306 $\delta^{202}\text{Hg}$ for GEM in background air is typically in the range of ≈-0.2 to 1.5‰ (Szponar et al., 2020 and
307 references therein). Foliar uptake of GEM is reported to cause substantial MDF of between -2.3 and -2.9‰
308 (Demers et al., 2013; Enrico et al., 2016; Wang et al., 2021). If we subtract the middle of the estimated range
309 of MDF caused by foliar uptake ($\delta^{202}\text{Hg}$: $-2.6 \pm 0.3 \text{‰}$) from the mean $\delta^{202}\text{Hg}$ values measured in tree rings
310 during 1^{st} IP and 2^{nd} IP we get $\delta^{202}\text{Hg}$ estimates of $-1.7 \pm 0.2 \text{‰}$ and $-1.4 \pm 0.2 \text{‰}$ (propagated uncertainty),
311 respectively, for GEM during these periods at the approximate location of the southeast facing forest stand
312 where the Spruce ISO trees were sampled (see also Fig. 4). This agrees with other studies that suggest
313 industrial sources of Hg are enriched in lighter isotopes compared to background air (Jiskra et al., 2019;
314 Szponar et al., 2020, and references therein). These estimates assume Hg in tree rings is derived from foliar
315 uptake of GEM from the atmosphere, which is suggested to be the dominant uptake pathway of Hg in trees
316 (e.g., Beauford et al., 1977; Graydon et al. 2009; Cozzolino et al., 2016), and no further MDF during
317 downward transport of Hg within the trees (as observed by Liu et al., 2021).

318 Applying the same correction to the $\delta^{202}\text{Hg}$ in tree rings from the BGP we get a $\delta^{202}\text{Hg}$ estimate of -0.2 ± 0.3
319 ‰ for GEM during this time (see also Fig. 4). This is right on the lower end of the reported range for $\delta^{202}\text{Hg}$
320 of typical background GEM and suggests there may still be some minor inputs of Hg from the still
321 contaminated soils (McLagan et al., 2022) to the trees during the BGP. GEM concentrations were measured
322 with PASs over the areas of the former kyanisation building and wood drying areas ($2.9 \pm 0.6 \text{ ng}\cdot\text{m}^{-3}$) and
323 concentrations were approximately double typical European background concentrations (≈ 1.5 — $2.0 \text{ ng}\cdot\text{m}^{-3}$)
324 (Sprovieri et al., 2016). Other studies that have observed more elevated GEM concentrations with co-located
325 GEM PAS deployments: up to three orders of magnitude higher concentrations at a former Hg mine
326 (McLagan et al., 2018) and 3—4x higher at a Hg contaminated waste site (McLagan et al., 2021b).
327 Therefore, we can assume the slightly elevated GEM concentrations detected at the site in 2018 are
328 associated with low-level GEM emission from the site. These minor emissions likely cause a small negative
329 shift in $\delta^{202}\text{Hg}$ values of the tree rings from what might be expected of “true” background values. To our
330 knowledge this is the first study to address elevated GEM concentrations from a former Hg kyanisation
331 facility.

332 3.2.2. Mass independent fractionation (MIF)

333 We also observed small variability in odd isotope-MIF in the Spruce ISO tree rings (Fig. 3B). The mean
334 $\Delta^{199}\text{Hg}$ for the 1^{st} IP ($\Delta^{199}\text{Hg}$: $0.00 \pm 0.03 \text{‰}$, 1SD) was significantly greater ($p < 0.001$) than for the 2^{nd} IP
335 ($\Delta^{199}\text{Hg}$: $-0.06 \pm 0.04 \text{‰}$, 1SD), which in turn was significantly greater ($p < 0.001$) than the BGP ($\Delta^{199}\text{Hg}$: $-$
336 $0.13 \pm 0.03 \text{‰}$, 1SD). The $\Delta^{199}\text{Hg}$ of the 1^{st} IP is right at the mean values for cinnabar ores ($\Delta^{199}\text{Hg}$: $0.01 \pm$
337 0.10‰ , 1SD) and liquid $\text{Hg}(0)$ stocks ($\Delta^{199}\text{Hg}$: $-0.01 \pm 0.03 \text{‰}$, 1SD) (Sun et al., 2016; Grigg et al., 2018).
338 Additionally, the mean $\Delta^{199}\text{Hg}$ values from the solid phase materials at this contaminated site
339 were $-0.01 \pm 0.06 \text{‰}$ (McLagan et al., 2022). Hence, we suggest $\Delta^{199}\text{Hg}$ values in the tree rings during 1^{st} IP
340 are conserved from the industrial activities.

341 Wang et al. (2021) made similar observations in Masson Pine tree rings near a former Hg mine in Guizhou
342 Province of China: more positive $\Delta^{199}\text{Hg}$ values during periods of more intense industrial activity. The more
343 negative $\Delta^{199}\text{Hg}$ values in tree rings from the BGP are similar to the more negative background GEM values

344 (typical range: -0.4 to 0.0 ‰; Szponar et al., 2020 and references therein). Scanlon et al. (2020) measured
345 low THg concentration (<4.5 $\mu\text{g}\cdot\text{kg}^{-1}$) in red oak, white oak, and pitch pine tree rings and negative $\Delta^{199}\text{Hg}$
346 values (-0.39 to -0.14 ‰) and also associated this with the characteristic GEM signature of background air.
347 The difference in $\Delta^{199}\text{Hg}$ between the *1stIP*, *2ndIP*, and *BGP* is likely related to the atmospheric mixing of
348 background GEM with industrially derived Hg. Foliar uptake has been reported to impart a small negative
349 $\Delta^{199}\text{Hg}$ shift (\approx -0.1 to -0.2 ‰; Demers et al., 2013; Yuan et al., 2018). Yet, our data were more indicative of
350 sources (industrial or background); thus, any negative $\Delta^{199}\text{Hg}$ shift may be small in Norway spruce and/or
351 differences fall within the range of variability of the sources.

352 Information on the specific processes driving odd-MIF (nuclear volume effect (NVE) vs magnetic isotope
353 effect (MIE)) in the measured Hg can be derived from the ratio of $\Delta^{199}\text{Hg}$ to $\Delta^{201}\text{Hg}$ (Bergquist and Blum,
354 2007; Blum et al., 2014). We derived a slope of 1.25 ± 0.13 (1SE) for bole wood using York orthogonal
355 regression (Fig. S8.1; York et al., 2004), which is higher than other studies (1.04 in Wang et al., 2021; and
356 1.05 in Scanlon et al., 2020 and Liu et al., 2021), but still lies in the range of the expected slope (1.0—1.3)
357 for MIE related photochemical reduction of Hg(II) to Hg(0) (Bergquist and Blum, 2007; Zheng et al., 2009).
358 The observed MIF data suggest MIE related photochemical reduction and subsequent Hg(0) evasion is likely
359 the dominant pathway of Hg(0) to the atmosphere. However, we caution against the over interpretation of
360 these data as there was a large difference in the slope using a different orthogonal regression method (Fig.
361 S8.1; Deming 1943). This difference in methods can largely be explained by the limited extent of odd-MIF
362 observed in the tree ring data.

363 Both, $\Delta^{200}\text{Hg}$ and $\Delta^{204}\text{Hg}$ values show there was no significant even isotope-MIF in the bole wood samples
364 (Section S8). $\Delta^{200}\text{Hg}$ anomalies have been reported for Hg in precipitation samples and related to upper
365 atmosphere oxidation of Hg(0) (Gratz et al., 2010; Chen et al., 2012). Thus, the near zero even-MIF supports
366 the hypothesis that the Hg in tree rings relates to foliar uptake of atmospheric GEM (unaffected by even-
367 MIF) rather than root uptake of Hg deposited to soils via wet deposition of Hg(II).

368 **3.3. Physiological and species related factors impacting within tree Hg cycling**

369 **3.3.1. THg concentration and stable Hg isotopes in bark**

370 THg concentrations in the bark of three Spruce ISO trees ($137 \pm 105 \mu\text{g}\cdot\text{kg}^{-1}$) were significantly higher than
371 THg in bole wood of *BGP* ($p = 0.014$), *2ndIP* ($p = 0.025$), and *1stIP* ($p = 0.042$). Furthermore, the bark was
372 divided into inner (younger) and outer (older) bark of Spruce ISO4 and ISO5 trees and the outer bark was 2.0
373 and 2.7x higher in THg concentrations, respectively. This is similar to the observations made by Chiarantini
374 et al. (2016) for black pine and could be related to longer and more exposure of the outer bark to elevated
375 atmospheric Hg concentrations leading to more Hg deposited to these layers. Nonetheless, the older, outer
376 bark would have been closer to the phloem (inner most bark layer; likely pathway for downward transport of
377 Hg in trees) during the *1stIP* and *2ndIP* when we expect GEM concentrations were much higher than they are
378 presently. Moreover, the inner bark concentrations (Spruce ISO4: $57.7 \mu\text{g}\cdot\text{kg}^{-1}$; Spruce ISO5: $163.1 \mu\text{g}\cdot\text{kg}^{-1}$)
379 were still elevated with reference to the *BGP* in particular. Arnold et al. (2018) and Peckham et al. (2019a)
380 suggest that translocation of Hg from the phloem into the inactive inner bark layers may be an important
381 source of Hg stored within bark, which they further suggest supports findings by Chiarantini et al. (2016)
382 that inner bark layers have a higher proportion of “organic Hg” than the outer layers in black pine.

383 If the predominant source of Hg in bark was via deposition of either GEM or GOM/PBM then we would
384 expect to observe more positive $\delta^{202}\text{Hg}$ values in the bark samples as this pathway is unaffected by the large
385 negative MDF (\approx -2.6 ‰) associated with stomatal uptake. However, the $\delta^{202}\text{Hg}$ values for the bark samples
386 were all highly negative ($\delta^{202}\text{Hg}$: $-3.90 \pm 0.30 \text{ ‰}$, 1SD) and similar to the highly negative values in tree ring
387 samples from the *1stIP* and *2ndIP*. Furthermore, GOM/PBM is reported to have more positive $\Delta^{199}\text{Hg}$ values

388 than GEM (Szponar et al., 2020), but the bark samples ($\Delta^{199}\text{Hg}$: $-0.14 \pm 0.06 \text{‰}$, 1SD) were similar if not
389 slightly more negative than the bole wood from these industrial periods (Fig. 4). There was very little
390 difference in $\delta^{202}\text{Hg}$ or $\Delta^{199}\text{Hg}$ between the inner and outer bark of either Spruce ISO4 or ISO5 tree (Table
391 S4.1). In summary, our Hg stable isotope data suggests the stomatal uptake, internal transport, and
392 translocation from phloem to inner bark is likely the dominant uptake pathway for Hg stored in bark. Liu et
393 al. (2021) posited the same foliage assimilation pathway for bark Hg uptake based on similar $\delta^{202}\text{Hg}$ and
394 $\Delta^{199}\text{Hg}$ values in both their bark and bole wood samples from subtropical evergreen species at a background
395 site. Considering rays that connect xylem and phloem reach as far as the inner bark (Nagy et al., 2014;
396 Pfautsch et al., 2015), this mechanism of bark Hg enrichment is a distinct possibility. More data across a
397 range of species, particularly using Hg stable isotopes, would be beneficial to determine the robustness of
398 this conclusion.

399 3.3.2. Sapwood (hydroactive xylem) rings enriched in Hg

400 THg concentrations were elevated in sapwood tree ring samples of all trees from both species, including
401 Spruce BG, compared to tree rings from the *BGP*. The 0—5 year samples were elevated in all trees and the
402 5—10 and 10—15 year samples were also higher in THg concentrations in some trees (Fig. 2). Although part
403 of the phloem (~~first layer of bark~~) may have been included in some 0—5 year samples and contributed to
404 enrichment of these samples, elevated THg concentrations in certain 5—10 and 10—15 year samples
405 indicate this is not the sole determinant. Sapwood enrichment has also been observed in both Norway spruce
406 (Hojdová et al., 2011) and European larch (Navrátil et al., 2018; Nováková et al., 2021; 2022) and various
407 species of oak and pine (Wright et al., 2014; Navrátil et al., 2017; Scanlon et al., 2020; Wang et al., 2021).
408 Our study represents perhaps the most pronounced and consistent (across all trees) example of this sapwood
409 enrichment. Nováková et al. (2021) suggest the tree coring sampling method could be a potential source of
410 this enrichment. However, we observe this in the Spruce ISO trees that were sampled by breaking up tree
411 “cookies” rather than coring, which would rule out this possibility.

412 We examine three alternate scenarios to explain this. The first is that GEM concentrations in the area have
413 been elevated during the last decade compared to the *BGP*. While the PAS measured GEM concentrations
414 were slightly elevated ($\approx 2x$ European background concentrations) likely associated with minor on-going
415 releases from contaminated topsoils, there is no evidence to suggest why GEM concentrations in the most
416 recent 5—10 years would be higher than the earlier *BGP*. Additionally, the Spruce BG tree also had elevated
417 THg concentrations in all samples under 15 years, which had little-to-no impact in tree ring Hg by the
418 industrial facility during *1stIP* or *2ndIP*. The European Monitoring and Evaluation Programme (EMEP) has a
419 long-term monitoring station $\approx 22\text{km}$ to the west of the former industrial site ($\approx 16.5\text{ km}$ west of Spruce BG)
420 and reports a mean total gaseous Hg (predominantly GEM) concentration of $1.49\text{ ng}\cdot\text{m}^{-3}$ ($\pm 0.24\text{ ng}\cdot\text{m}^{-3}$
421 measurement uncertainty; $\pm 0.12\text{ ng}\cdot\text{m}^{-3}$ SD of annual means) over the last decade (EMEP, 2022), which is a
422 typical background concentration for Europe (Sprovieri et al., 2016). Hence, recently elevated GEM
423 concentrations cannot explain the elevated sapwood THg concentrations.

424 The second would relate to uptake of Hg from tree roots. The conductive or actively transporting component
425 of xylem (hydroactive xylem) exists within the sapwood of trees. Its primary role is the upward transport of
426 water and nutrients from tree roots to the aerial components and particularly leaves/needles. We have already
427 discussed how this pathway has been shown to be a minor mechanism of Hg uptake in many studies (e.g.,
428 Beauford et al., 1977; Graydon et al. 2009; Cozzolino et al., 2016). Also, the sampled trees are outside the
429 area in which surface contamination from the industrial activity occurred (particularly Spruce BG); any soil
430 contamination must have come from atmospheric Hg emissions and subsequent deposition, of which
431 stomatal uptake of GEM is the dominant conduit in forest ecosystems (Obrist et al., 2017; 2018; Jiskra et al.,
432 2018). We consider this mechanism highly unlikely to be driving sapwood enrichment.

433 The third scenario relates to tree physiology. Hg is transported downwards in trees via the phloem and has
434 been reported to translocate from phloem to xylem (sapwood) throughout this process (Arnold et al., 2018;
435 Yanai et al., 2020; Nováková et al., 2021). As sapwood ages it undergoes a physiological transition to
436 heartwood, which is drier, contains predominantly dead cells, and is used for structure rather than transport
437 (Bertaud and Holmbom, 2004; Metsä-Kortelainen et al., 2006). Hg that remains in the tree rings after the
438 transition to heartwood likely binds to components that endure this change, but there is a caveat in our
439 knowledge of this process (Yanai et al., 2020; Nováková et al., 2021). Since we use dry weight THg
440 concentrations, if all the Hg translocated from phloem to xylem was conserved in the wood during the
441 transition from sapwood to heartwood, then we would not expect to see any sapwood enrichment. Thus, we
442 deem it likely that some fraction of Hg is retained in the xylem solution or structures/chemicals enhanced in
443 sapwood (compared to heartwood) of these species. Although we only have two samples from the 0–5 year
444 tree rings analysed for stable isotopes, the $\delta^{202}\text{Hg}$ data from Spruce ISO5 and ISO-6 are shifted negative (-
445 0.41 and -0.33 ‰, respectively) in these samples compared to the adjacent composite sample of tree rings in
446 each respective tree (Fig. 3A; Section S6). Hence, the process controlling retention of this Hg in sapwood
447 would seem to favour lighter isotopes, implying there could be either preferential retention of specific Hg-
448 compounds or a change in binding form during the retention process.

449 Any upwards transport of xylem solution Hg may contribute to the slightly elevated THg concentrations that
450 Yanai et al. (2020) observed in tree rings at higher elevations above the ground. Sapwood is also a storage
451 reserve for energy (starch) and water (Taylor et al., 2002); therefore, some of the Hg in xylem solution may
452 be stored long-term in the hydroactive xylem without being transferred as the sapwood rings transition to
453 heartwood. While long-term storage of some Hg in sapwood could be a factor driving temporal differences
454 between tree ring THg concentrations and reported industrial activity in the literature (Arnold et al., 2018;
455 Wang et al., 2021), our data do not reflect such Hg translocation. Ultimately, further research will be needed,
456 particularly using Hg stable isotopes, to further explore this hypothesis and the physiological mechanisms
457 behind this enrichment.

458 3.3.3. The impact of species on uptake and storage of Hg in tree rings

459 There is extensive discussion in the literature on species specific differences in THg concentrations of tree
460 rings, particularly as they relate to foliar uptake rates (Wohlgemuth et al., 2020) and inter-ring translocation
461 (Arnold et al., 2018; O'Connor et al., 2019). Inter-ring translocation has led some studies to question the
462 overall effectiveness using tree rings as an archive for atmospheric GEM, but many of these studies have
463 utilised oak (Scanlon et al., 2020), some pine species (Wang et al., 2021; Nováková et al., 2021), and
464 *Populus* (Arnold et al., 2018). Certain physiological characteristics of these species (i.e., more radially
465 conductive xylem) that enhance this translocation may limit their applicability to tree ring atmospheric
466 archiving (Arnold et al., 2018; Nováková et al., 2021; Gustine et al., 2022). Several studies have observed
467 strong correlations between THg concentrations in spruce (Hojdová et al., 2011) and larch (Navrátil et al.,
468 2018; Nováková et al., 2021) tree rings and reported industrial activities and suggest these to be appropriate
469 species for archiving atmospheric GEM concentrations.

470 Despite the quite apparent physiological differences between European larch (deciduous conifer) and
471 Norway spruce (evergreen conifer), trends in THg concentrations varied little between the sampled trees of
472 either species. Sapwood was enriched, *BGP* THg was low, and concentrations increased into the 2ndIP at the
473 same time (early 1990s) in both larch and spruce trees (all sampled larch were planted after the 1stIP) (Fig.
474 2). Additionally, the good correlation between changes in THg concentrations and the timelines of the 1stIP,
475 2ndIP, and *BGP* suggest the process driving sapwood Hg enrichment results in limited inter-ring Hg
476 translocation in Norway spruce and European larch; the fraction of Hg transferred to heartwood must be
477 relatively consistent under this scenario. Thus, our data too suggest Norway spruce and European larch are
478 effective species for the chronicling of historic GEM concentrations.

479 **3.3.4. Between and within tree variability in tree ring Hg**

480 Heterogeneity in the radial distribution of Hg has been observed in other studies and authors suggest
481 sampling of multiple trees in each stand and different radial sections of trees provides more representative
482 assessments (Wright et al., 2014; Peckham et al., 2019b). The sampling direction of the bole or height of the
483 sampling can cause differences within replicate samples from the same tree. Factors affecting between tree
484 variability include microtopography, tree age or species and related specific physiological differences such
485 as photosynthesis rate, stomatal conductance and transpiration (Binda et al., 2021). No correlation between
486 Hg concentration and tree core mass was reported by Scanlon et al. (2020) and they concluded that
487 differences in radial growth do not dilute or concentrate Hg in tree rings. These authors therefore concluded
488 that Hg concentrations are a suitable proxy to evaluate trends of GEM. We detected some variability in THg
489 concentrations between Spruce ISO4, ISO5, and ISO6 from the same stand of trees (Fig. 2) and in
490 “replicated” tree rings from different sides of the Spruce ISO tree slices (mean relative difference: 78 ± 35
491 %; mean absolute difference: $5 \pm 5 \mu\text{g}\cdot\text{kg}^{-1}$; $n = 10$; Table S3.1). Yet, variability in the ratios of Hg stable
492 isotopes within the bole wood was low (mean absolute difference: $\delta^{202}\text{Hg}: 0.11 \pm 0.08 \text{‰}$ 1SD; $\Delta^{199}\text{Hg}: 0.08$
493 $\pm 0.02 \text{‰}$ 1SD; $n = 4$; Table S4.2). This suggests factors influencing radial Hg heterogeneity cause little
494 impact of Hg stable isotopes. We considered the stable isotopes analyses based on combined data from all
495 three trees, but individual trees also followed these trends (Section S6).

496 **Data availability**

497 All data are available within the paper and supplementary information. If there are any additional requests,
498 please contact the authors.

499 **Supplementary information**

500 The Supporting Information is available free of charge at DOI: XXX.

501 **Author Contribution**

502 The project design and planning were made by DSM and LS, with inputs from TN. The manuscript was
503 written predominantly by DSM with inputs from LS. Figures were prepared by DSM and LS. Supplemental
504 information was prepared predominantly by LS with inputs from DSM. Tree core sampling was performed
505 by DSM and LS, HB collected tree slices/“cookies”. THg analyses were performed by LS and DSM, passive
506 samplers were analysed by DSM, pre-concentration and isotope analysis was performed by LS. Lab space
507 provided by HB and SMK. DSM, LS, HB, and TN contributed to manuscript reviews. DSM and LS
508 contributed equally to this work.

509 **Conflicts of Interest**

510 The authors declare no competing financial interest.

511 **Acknowledgements**

512 We would like to acknowledge Herwig Lenitz, Petra Schmidt, and Adelina Calean for analytical assistance
513 and discussions with analysis, Sofie M. Reiter for the assistance with the pre-concentration of the isotope
514 samples, Jan Wiederhold for discussion on data, Jan Pietrucha for help assessing site reports and assistance
515 in analysis, Matthias Beyer for use of the increment borer. This research was funded by the German
516 Research Foundation (DFG) grant BI 734/17-1 and the Austrian Science Fund (FWF) grant I-3489-N28.

517 **References**

518 Abreu, S. N., Soares, A. M. V. M., Nogueira, A. J. A., and Morgado, F.: Tree rings, *Populus nigra* L.; as
519 mercury data logger in aquatic environments: Case study of an historically contaminated environment, *Bull.*
520 *Environ. Contam. Toxicol.*, 80(3), 294-299. DOI: 10.1007/s00128-008-9366-0, 2008.

521 Arnold, J., Gustin, M. S., and Weisberg, P. J.: Evidence for nonstomatal uptake of Hg by aspen and
522 translocation of Hg from foliage to tree rings in Austrian pine, *Environ. Sci Technol.*, 52(3), 1174-1182,
523 DOI: 10.1021/acs.est.7b04468, 2018.

524 Beauford, W., Barber, J., and Barringer, A. R.: Uptake and distribution of mercury within higher plants,
525 *Physiol. Plant.*, 39(4), 261-265, DOI: 10.1111/j.1399-3054.1977.tb01880.x, 1977.

526 Becnel, J., Falgeust, C., Cavalier, T., Gauthreaux, K., Landry, F., Blanchard, M., Beck, M. J., and Beck, J.N.:
527 Correlation of mercury concentrations in tree core and lichen samples in southeastern Louisiana, *Microchem.*
528 *J.*, 78(2), 205-210, DOI: 10.1016/j.microc.2004.06.002, 2004.

529 Bergquist, B. A., and Blum, J. D.: Mass-dependent and-independent fractionation of Hg isotopes by
530 photoreduction in aquatic systems, *Sci.*, 318(5849), 417-420, DOI: 10.1126/science.1148050, 2007.

531 Bergquist, B. A., and Blum, J. D.: The odds and evens of mercury isotopes: applications of mass-dependent
532 and mass-independent isotope fractionation, *Elements*, 5(6), 353-357, DOI: 10.2113/gselements.5.6.353,
533 2009.

534 Berta, F., and Holmbom, B.: Chemical composition of earlywood and latewood in Norway spruce
535 heartwood, sapwood and transition zone wood, *Wood Sci. Technol.*, 38(4), 245-256, DOI: 10.1007/s00226-
536 004-0241-9, 2004.

537 Binda, G., Di Lorio, A., and Monticelli, D.: The what, how, why, and when of dendrochemistry:
538 (paleo)environmental information from the chemical analysis of tree rings, *Sci. Tot. Environ.*, 758, 143672,
539 DOI: 10.1016/j.scitotenv.2020.143672, 2021.

540 Bishop, K. H., Lee, Y. H., Munthe, J., and Dambrine, E.: Xylem sap as a pathway for total mercury and
541 methylmercury transport from soils to tree canopy in the boreal forest, *Biogeochem.*, 40(2), 101-113, DOI:
542 10.1023/A:1005983932240, 1998.

543 Blum, J. D., Sherman, L. S., and Johnson, M. W.: Mercury isotopes in earth and environmental sciences,
544 *Annu. Rev. Earth Planet. Sci.*, 42, 249-269, DOI: 10.1146/annurev-earth-050212-124107, 2014.

545 Browne, C. L., and Fang, S. C.: Uptake of mercury vapor by wheat: an assimilation model, *Plant Physiol.*,
546 61(3), 430-433, DOI: 10.1104/pp.61.3.430, 1978.

547 Chen, J., Hintelmann, H., Feng, X., and Dimock, B.: Unusual fractionation of both odd and even mercury
548 isotopes in precipitation from Peterborough, ON, Canada, *Geochim. Cosmochim. Acta*, 90, 33-46, DOI:
549 10.1016/j.gca.2012.05.005, 2012.

550 Chiarantini, L., Rimondi, V., Benvenuti, M., Beutel, M. W., Costagliola, P., Gonnelli, C., Lattanzi, P., and
551 Paolieri, M.: Black pine (*Pinus nigra*) barks as biomonitor of airborne mercury pollution, *Sci. Total*
552 *Environ.*, 569, 105-113, DOI: 10.1016/j.scitotenv.2016.06.029, 2016.

553 Chiarantini, L., Rimondi, V., Bardelli, F., Benvenuti, M., Cosio, C., Costagliola, P., Di Benedetto, F.,
554 Lattanzi, P., and Sarret, G.: Mercury speciation in *Pinus nigra* barks from Monte Amiata (Italy): An X-ray
555 absorption spectroscopy study, *Environ. Pollut.*, 227, 83-88, DOI: 10.1016/j.envpol.2017.04.038, 2017.

556 Clackett, S. P., Porter, T. J., and Lehnher, I.: 400-year record of atmospheric mercury from tree-rings in
557 Northwestern Canada, *Environ. Sci. Technol.*, 52(17), 9625-9633, DOI: 10.1021/acs.est.8b01824, 2018.

558 Cozzolino, V., De Martino, A., Nebbioso, A., Di Meo, V., Salluzzo, A., and Piccolo, A.: Plant tolerance to
559 mercury in a contaminated soil is enhanced by the combined effects of humic matter addition and inoculation
560 with arbuscular mycorrhizal fungi, *Environ. Sci. Pollut. Res.*, 23(11), 11312-11322, DOI: 10.1007/s11356-
561 016-6337-6, 2016.

562 Cui, L., Feng, X., Lin, C. J., Wang, X., Meng, B., Wang, X., and Wang, H.: Accumulation and translocation
563 of 198Hg in four crop species, *Environ. Toxicol. Chem.*, 33(2), 334-340, DOI: 10.1002/etc.2443, 2014.

564 Cutter, B. E., and Guyette, R. P.: Anatomical, chemical, and ecological factors affecting tree species choice
565 in dendrochemistry studies, *J. Environ. Qual.*, 22(3), 611-619, DOI:
566 10.2134/jeq1993.00472425002200030028x, 1993.

567 Dastoor, A., Angot, H., Bieser, J., Christensen, J., Douglas, T., Heimbürger-Boavida, L. E., Jiskra, M.,
568 Mason, R., McLagan, D. S., Obrist, D., Outridge, P., Petrova, M., Ryjkov, A., St. Pierre, K., Schartup, A.,
569 Soerensen, A., Travnikov, O., Toyota, K., Wilson, S., and Zdanowicz, C.: Arctic mercury cycling, *Nat. Rev. Earth Environ.*, 3, 270-286, DOI: 10.1038/s43017-022-00269-w, 2022.

571 Demers, J. D., Blum, J. D., and Zak, D. R.: Mercury isotopes in a forested ecosystem: Implications for air-
572 surface exchange dynamics and the global mercury cycle, *Global Biogeochem. Cy.*, 27(1), 222-238, DOI:
573 10.1002/gbc.20021, 2013.

574 Deming, W. E.: *Statistical adjustment of data*. Wiley, New Jersey, USA, 1943.

575 Dennis, K. K., Uppal, K., Liu, K. H., Ma, C., Liang, B., Go, Y. M., and Jones, D. P.: Phytochelatin database:
576 a resource for phytochelatin complexes of nutritional and environmental metals, *Database*, 2019, baz083,
577 DOI: 10.1093/database/baz083, 2019.

578 Eisele, G.: Arbeitshilfe Absicherbarkeit von Risiken beim Flächenrecycling, *Forschungsbericht FZKA-BWPLUS*,
579 Landesanstalt für Umwelt Baden-Württemberg, Baden-Württemberg, Germany, 102.
580 <https://pd.lubw.de/99447>, 2004.

581 EMEP: Co-operative Programme for Monitoring and Evaluation of the Long-Range Transmissions of Air
582 Pollutants in Europe, European Monitoring and Evaluation Programme (EMEP), Kjeller, Norway.
583 <https://projects.nilu.no/ccc/reports.html>, accessed: Feb 09, 2022, 2022.

584 Enrico, M., Roux, G. L., Maruscak, N., Heimbürger, L. E., Claustres, A., Fu, X., Sun, R., and Sonke, J. E.:
585 Atmospheric mercury transfer to peat bogs dominated by gaseous elemental mercury dry deposition,
586 *Environ. Sci. Technol.*, 50(5), 2405-2412, DOI: 10.1021/acs.est.5b06058, 2016.

587 Friedli, H. R., Arellano, A. F., Cinnirella, S., and Pirrone, N.: Initial estimates of mercury emissions to the
588 atmosphere from global biomass burning, *Environ. Sci. Technol.*, 43(10), 3507-3513, DOI:
589 10.1021/es802703g, 2009.

590 Gratz, L. E., Keeler, G. J., Blum, J. D., and Sherman, L. S.: Isotopic composition and fractionation of
591 mercury in Great Lakes precipitation and ambient air, *Environ. Sci. Technol.*, 44(20), 7764-7770, DOI:
592 10.1021/es100383w, 2010.

593 Graydon, J. A., St. Louis, V. L., Hintelmann, H., Lindberg, S. E., Sandilands, K. A., Rudd, J. W., Kelly, C.
594 A., Tate, M. T., Krabbenhoft, D. P., and Lehnher, I.: Investigation of uptake and retention of atmospheric
595 Hg (II) by boreal forest plants using stable Hg isotopes, *Environ. Sci. Technol.*, 2009, 43(13), 4960-4966,
596 DOI: 10.1021/es900357s, 2009.

597 Grigg, A. R., Kretzschmar, R., Gilli, R. S., and Wiederhold, J. G.: Mercury isotope signatures of digests and
598 sequential extracts from industrially contaminated soils and sediments. *Sci. Total Environ.*, 2018, 636, 1344-
599 1354, DOI: 10.1016/j.scitotenv.2018.04.261, 2018.

600 Gustin, M. S., Ingle, B., and Dunham-Cheatham, S. M.: Further investigations into the use of tree rings as
601 archives of atmospheric mercury concentrations, *Biogeochem.*, 158, 167-180, DOI: 10.1007/s10533-022-
602 00892-1, 2022.

603 Hojlová, M., Navrátil, T., Rohovec, J., Žák, K., Vaněk, A., Chrastný, V., Bače, R., and Svoboda, M.:
604 Changes in mercury deposition in a mining and smelting region as recorded in tree rings, *Water Air Soil
605 Pollut.*, 216(1), 73-82, DOI: 10.1007/s11270-010-0515-9, 2011.

606 Jiskra, M., Wiederhold, J. G., Skjellberg, U., Kronberg, R. M., Hajdas, I., and Kretzschmar, R.: Mercury
607 deposition and re-emission pathways in boreal forest soils investigated with Hg isotope signatures, *Environ.
608 Sci Technol.*, 49(12), 7188-7196, DOI: 10.1021/acs.est.5b00742, 2015.

609 Jiskra, M., Sonke, J. E., Obrist, D., Bieser, J., Ebinghaus, R., Myhre, C. L., Pfaffhuber, K. A., Wängberg, I.,
610 Kyllönen, K., Worthy, D., and Martin, L. G.: A vegetation control on seasonal variations in global
611 atmospheric mercury concentrations, *Nature Geosci.*, 11(4), 244-250, DOI: 10.1038/s41561-018-0078-8,
612 2018.

613 Jiskra, M., Maruszak, N., Leung, K. H., Hawkins, L., Prestbo, E., and Sonke, J. E.: Automated stable
614 isotope sampling of gaseous elemental mercury (ISO-GEM): Insights into GEM emissions from building
615 surfaces, *Environ. Sci Technol.*, 53(8), 4346-4354, DOI: 10.1021/acs.est.8b06381, 2019.

616 Kahle, H.: Response of roots of trees to heavy metals, *Environ. Exp. Bot.*, 33(1), 99–119, DOI:
617 10.1016/0098-8472(93)90059-o, 1993.

618 Khan, T. R., Obrist, D., Agnan, Y., Selin, N. E., and Perlinger, J. A.: Atmosphere-terrestrial exchange of
619 gaseous elemental mercury: parameterization improvement through direct comparison with measured
620 ecosystem fluxes, *Environ. Sci. Process. Impacts*, 21(10), 1699-1712, DOI: 10.1039/C9EM00341J, 2019.

621 Laacouri, A., Nater, E. A., and Kolka, R. K.: Distribution and uptake dynamics of mercury in leaves of
622 common deciduous tree species in Minnesota, USA, *Environ. Sci Technol.*, 47(18), 10462-10470, DOI:
623 10.1021/es401357z, 2013.

624 Lin, C. J., and Pehkonen, S. O.: The chemistry of atmospheric mercury: a review, *Atmos. Environ.*, 33(13),
625 2067-2079, DOI: 10.1016/S1352-2310(98)00387-2, 1999.

626 Lindberg, S. E., Jackson, D. R., Huckabee, J. W., Janzen, S. A., Levin, M. J., and Lund, J. R.: Atmospheric
627 emission and plant uptake of mercury from agricultural soils near the Almaden mercury mine, *J. Environ.
628 Qual.*, 8(4), 572-578, DOI: 10.2134/jeq1979.00472425000800040026x, 1979.

629 Lindberg, S., Bullock, R., Ebinghaus, R., Engstrom, D., Feng, X., Fitzgerald, W., Pirrone, N., Prestbo, E.,
630 and Seigneur, C.: A synthesis of progress and uncertainties in attributing the sources of mercury in
631 deposition, *Ambio*, 36(1), 19-32, <http://www.jstor.org/stable/4315781>, 2007.

632 Liu, Y., Lin, C. J., Yuan, W., Lu, Z., and Feng, X.: Translocation and distribution of mercury in biomasses
633 from subtropical forest ecosystems: Evidence from stable mercury isotopes, *Acta Geochim.*, 40(1), 42-50,
634 DOI: 10.1007/s11631-020-00441-3, 2021.

635 Mao, H., and Talbot, R.: Speciated mercury at marine, coastal, and inland sites in New England–Part 1:
636 Temporal variability, *Atmos. Chem. Phys.*, 12(11), 5099-5112, DOI: 10.5194/acp-12-5099-2012, 2012.

637 McLagan, D. S., Monaci, F., Huang, H., Lei, Y. D., Mitchell, C. P. J., and Wania, F.: Characterization and
638 quantification of atmospheric mercury sources using passive air samplers. *J. Geophys. Res. Atmos.*, 124(4),
639 2351-2362, DOI: 10.1029/2018JD029373, 2019.

640 McLagan, D. S., Stupple, G. W., Darlington, A., Hayden, K., and Steffen, A.: Where there is smoke there is
641 mercury: Assessing boreal forest fire mercury emissions using aircraft and highlighting uncertainties
642 associated with upscaling emissions estimates, *Atmos. Chem. Phys.*, 21(7), 5635-5653, DOI: 10.5194/acp-
643 21-5635-2021, 2021a.

644 McLagan, D. S., Osterwalder, S., and Biester, H.: Temporal and spatial assessment of gaseous elemental
645 mercury concentrations and emissions at contaminated sites using active and passive measurements,
646 *Environ. Res. Commun.*, 3(5), p.051004, DOI: 10.1088/2515-7620/abfe02/meta, 2021b.

647 McLagan, D. S., Schwab, L., Wiederhold, J. G., Chen, L., Pietrucha, J., Kraemer, S. M., and Biester, H.:
648 Demystifying mercury geochemistry in contaminated soil–groundwater systems with complementary
649 mercury stable isotope, concentration, and speciation analyses, *Environ. Sci. Process. Impacts*, DOI:
650 10.1039/D1EM00368B, 2022.

651 Metsä-Kortelainen, S., Antikainen, T., and Viitaniemi, P.: The water absorption of sapwood and heartwood
652 of Scots pine and Norway spruce heat-treated at 170 C, 190 C, 210 C and 230 C, *Holz als Roh-und*
653 *Werkstoff*, 64(3), 192-197, DOI: 10.1007/s00107-005-0063-y, 2006.

654 Millhollen, A. G., Gustin, M. S., and Obrist, D.: Foliar mercury accumulation and exchange for three tree
655 species, *Environ. Sci Technol.*, 40(19), 6001-6006, DOI: 10.1021/es0609194, 2006.

656 Moreno, F. N., Anderson, C. W., Stewart, R. B., Robinson, B. H., Ghomshei, M., and Meech, J. A.: Induced
657 plant uptake and transport of mercury in the presence of sulphur-containing ligands and humic acid. *New*
658 *Phytol.*, 166(2), 445-454, DOI: 10.1111/j.1469-8137.2005.01361.x, 2005.

659 Moreno-Jiménez, E., Gamarra, R., Carpeta-Ruiz, R. O., Millán, R., Peñalosa, J. M., and Esteban, E.:
660 Mercury bioaccumulation and phytotoxicity in two wild plant species of Almadén area, *Chemosphere*,
661 63(11), 1969-1973, DOI: 10.1016/j.chemosphere.2005.09.043, 2006.

662 Mowat, L. D., St. Louis, V. L., Graydon, J. A., and Lehnherr, I.: Influence of forest canopies on the
663 deposition of methylmercury to boreal ecosystem watersheds, *Environ. Sci Technol.*, 45(12), 5178-5185,
664 DOI: 10.1021/es104377y, 2011.

665 Nagy, N. E., Sikora, K., Krokene, P., Hietala, A. M., Solheim, H., and Fossdal, C. G.: Using laser micro-
666 dissection and qRT-PCR to analyze cell type-specific gene expression in Norway spruce phloem, *PeerJ*, 2,
667 e362, DOI: 10.7717/peerj.362, 2014.

668 Navrátil, T., Šimeček, M., Shanley, J. B., Rohovec, J., Hojdrová, M., and Houška, J.: The history of mercury
669 pollution near the Spolana chlor-alkali plant (Neratovice, Czech Republic) as recorded by Scots pine tree
670 rings and other bioindicators, *Sci. Total Environ.*, 586, 1182-1192, DOI: 10.1016/j.scitotenv.2017.02.112,
671 2017.

672 Navrátil, T., Nováková, T., Shanley, J. B., Rohovec, J., Matoušková, S., Vaňková, M., and Norton, S. A.:
673 Larch tree rings as a tool for reconstructing 20th century Central European atmospheric mercury trends,
674 *Environ. Sci Technol.*, 52(19), 11060-11068, DOI: 10.1021/acs.est.8b02117, 2018.

675 Nováková, T., Navrátil, T., Demers, J. D., Roll, M., and Rohovec, J.: Contrasting tree ring Hg records in two
676 conifer species: Multi-site evidence of species-specific radial translocation effects in Scots pine versus
677 European larch, *Sci. Total Environ.*, 762, 144022, DOI: 10.1016/j.scitotenv.2020.144022, 2021.

678 Nováková T., Navrátil T., Schütze M., Rohovec J., Matoušková Š., Hošek M., Matys Grygar T.:
679 Reconstructing atmospheric Hg levels near the oldest chemical factory in central Europe using a tree ring
680 archive, *Environ. Pollut.*, 304, 119215, DOI: 10.1016/j.envpol.2022.119215, 2022.

681 Obrist, D., Agnan, Y., Jiskra, M., Olson, C. L., Colegrove, D. P., Hueber, J., Moore, C. W., Sonke, J. E., and
682 Helmig, D.: Tundra uptake of atmospheric elemental mercury drives Arctic mercury pollution, *Nature*,
683 547(7662), 201-204, DOI: 10.1038/nature22997, 2017.

684 Obrist, D., Kirk, J. L., Zhang, L., Sunderland, E. M., Jiskra, M., and Selin, N. E.: A review of global
685 environmental mercury processes in response to human and natural perturbations: Changes of emissions,
686 climate, and land use, *Ambio*, 47(2), 116-140, DOI: 10.1007/s13280-017-1004-9, 2018.

687 Odabasi, M., Tolunay, D., Kara, M., Falay, E. O., Tuna, G., Altıok, H., Dumanoglu, Y., Bayram, A., and
688 Elbir, T.: Investigation of spatial and historical variations of air pollution around an industrial region using
689 trace and macro elements in tree components, *Sci. Total Environ.*, 550, 1010-1021, DOI:
690 10.1016/j.scitotenv.2016.01.197, 2016.

691 O'Connor, D., Hou, D., Ok, Y. S., Mulder, J., Duan, L., Wu, Q., Wang, S., Tack, F. M., and Rinklebe, J.:
692 Mercury speciation, transformation, and transportation in soils, atmospheric flux, and implications for risk
693 management: A critical review, *Environ. Int.*, 126, 747-761, DOI: 10.1016/j.envint.2019.03.019, 2019.

694 Peckham, M. A., Gustin, M. S., Weisberg, P. J., and Weiss-Penzias, P.: Results of a controlled field
695 experiment to assess the use of tree tissue concentrations as bioindicators of air Hg, *Biogeochem.*, 142(2),
696 265-279, DOI: 10.1007/s10533-018-0533-z, 2019a.

697 Peckham, M. A., Gustin, M. S., and Weisberg, P. J.: Assessment of the suitability of tree rings as archives of
698 global and regional atmospheric mercury pollution, *Environ. Sci Technol.*, 53(7), 3663-3671, DOI:
699 10.1021/acs.est.8b06786, 2019b.

700 Peralta-Videa, J. R., Lopez, M. L., Narayan, M., Saupe, G., and Gardea-Torresdey, J.: The biochemistry of
701 environmental heavy metal uptake by plants: implications for the food chain, *Int. J. Biochem. Cell Biol.*,
702 41(8-9), 1665-1677, DOI: 10.1016/j.biocel.2009.03.005, 2009.

703 Pfautsch, S., Hölttä, T., and Mencuccini, M.: Hydraulic functioning of tree stems—fusing ray anatomy,
704 radial transfer and capacitance, *Tree Physiol.*, 35(7), 706-722, DOI: 10.1093/treephys/tpv058, 2015.

705 Rea, A. W., Lindberg, S. E., and Keeler, G. J.: Assessment of dry deposition and foliar leaching of mercury
706 and selected trace elements based on washed foliar and surrogate surfaces. *Environ. Sci Technol.*, 34(12),
707 2418-2425, DOI: 10.1021/es991305k, 2000.

708 Rea, A. W., Lindberg, S. E., and Keeler, G. J.: Dry deposition and foliar leaching of mercury and selected
709 trace elements in deciduous forest throughfall. *Atmos. Environ.*, 35(20), 3453-3462, DOI: 10.1016/S1352-
710 2310(01)00133-9, 2001.

711 Rea, A. W., Lindberg, S. E., Scherbatskoy, T., and Keeler, G. J.: Mercury accumulation in foliage over time
712 in two northern mixed-hardwood forests. *Water Air Soil Pollut.*, 133(1), 49-67, DOI:
713 10.1023/A:1012919731598, 2002.

714 Richard, J. H., Bischoff, C., Ahrens, C. G., and Biester, H.: Mercury (II) reduction and co-precipitation of
715 metallic mercury on hydrous ferric oxide in contaminated groundwater, *Sci. Total Environ.*, 539, 36-44,
716 DOI: 10.1016/j.scitotenv.2015.08.116, 2016.

717 Scanlon, T. M., Riscassi, A. L., Demers, J. D., Camper, T. D., Lee, T. R., and Druckenbrod, D. L.: Mercury
718 accumulation in tree rings: observed trends in quantity and isotopic composition in Shenandoah National

719 Park, Virginia, *J. Geophys. Res. Biogeosci.*, 125(2), p.e2019JG005445, DOI: 10.1029/2019JG005445, 2020.

720 Schrenk, V., and Hiester, U.: Analysis of Subsurface Remediation Technologies for Brownfield
721 Redevelopments, REVIT: revitalising industrial sites, City of Stuttgart, Stuttgart, Germany, P042/0702, 97.
722 https://www.researchgate.net/publication/283082200_Analysis_of_Subsurface
723 _Remediation_Technologies_for_Brownfield_Redevelopments, 2007.

724 Schroeder, W. H., and Munthe, J.: Atmospheric mercury—an overview. *Atmos. Environ.*, 32(5), 809-822,
725 DOI: 10.1016/S1352-2310(97)00293-8, 1998.

726 Selin, N. E.: Global biogeochemical cycling of mercury: a review, *Annu. Rev. Environ. Resour.*, 34, 43-63,
727 DOI: 10.1146/annurev.environ.051308.084314, 2009.

728 Selin, N. E., Jacob, D. J., Yantosca, R. M., Strode, S., Jaeglé, L., and Sunderland, E. M.: Global 3-D land-
729 ocean-atmosphere model for mercury: Present-day versus preindustrial cycles and anthropogenic enrichment
730 factors for deposition, *Global Biogeochem. Cy.*, 22(2), GB2011, DOI: 10.1029/2007GB003040, 2008.

731 Siwik, E. I., Campbell, L. M., and Mierle, G.: Distribution and trends of mercury in deciduous tree cores,
732 *Environ. Pollut.*, 158(6), 2067-2073, DOI: 10.1016/j.envpol.2010.03.002, 2010.

733 Sprovieri, F., Pirrone, N., Bencardino, M., D'Amore, F., Carbone, F., Cinnirella, S., Mannarino, V., Landis,
734 M., Ebinghaus, R., Weigelt, A., Brunke, E.G., Labuschagne, C., Martin, L., Munthe, J., Wängberg, I.,
735 Artaxo, P., Morais, F., de Melo Jorge Barbosa, H., Brito, J., Cairns, W., Barbante, C., del Carmen Diéguez,
736 M., Garcia P. E., Dommergue, A., Angot, H., Magand, O., Skov, H., Horvat, M., Kotnik, J., Read, K. A.,
737 Mendes Neves, L., Gawlik, B. M., Sena, F., Mashyanov, N., Obolkin, V., Wip, D., Feng, X. B., Zhang, H.,
738 Fu, X., Ramachandran, R., Cossa, D., Knoery, J., Maruszczak, N., Nerentorp, M., and Norstrom C.:
739 Atmospheric mercury concentrations observed at ground-based monitoring sites globally distributed in the
740 framework of the GMOS network, *Atmos. Chem. Phys.*, 16(18), 11915-11935, DOI: 10.5194/acp-16-11915-
741 2016, 2016.

742 Sun, R., Streets, D. G., Horowitz, H. M., Amos, H. M., Liu, G., Perrot, V., Toutain, J. P., Hintelmann, H.,
743 Sunderland, E. M., Sonke, J. E., and Blum, J. D.: Historical (1850–2010) mercury stable isotope inventory
744 from anthropogenic sources to the atmosphere. *Elementa Sci. Anthropocene*, 2016, 4, 91.

745 Szponar, N., McLagan, D. S., Kaplan, R. J., Mitchell, C. P., Wania, F., Steffen, A., Stupple, G. W., Monaci,
746 F., and Bergquist, B. A.: Isotopic characterization of atmospheric gaseous elemental mercury by passive air
747 sampling, *Environ. Sci Technol.*, 54(17), 10533-10543, DOI: 10.12952/journal.elementa.000091, 2020.

748 Taylor, A. M., Gartner, B. L., and Morrell, J. J.: Heartwood formation and natural durability-a review. *Wood*
749 *Fibre Sci.*, 2002, 34(4), 587-611.

750 Wang, X., Luo, J., Yin, R., Yuan, W., Lin, C.J., Sommar, J., Feng, X., Wang, H., and Lin, C.: Using mercury
751 isotopes to understand mercury accumulation in the montane forest floor of the Eastern Tibetan Plateau.
752 *Environ. Sci Technol.*, 2017, 51(2), 801-809.

753 Wang, X., Yuan, W., Lin, C. J., Luo, J., Wang, F., Feng, X., Fu, X., and Liu, C.: Underestimated sink of
754 atmospheric mercury in a deglaciated forest chronosequence, *Environ. Sci Technol.*, 54(13), 8083-8093,
755 DOI: 10.1021/acs.est.0c01667, 2020.

756 Wang, X., Yuan, W., Lin, C. J., Wu, F., and Feng, X.: Stable mercury isotopes stored in Masson Pinus tree
757 rings as atmospheric mercury archives, *J. Hazard. Mater.*, 415, 125678, DOI:
758 10.1016/j.hazmat.2021.125678, 2021.

759 Weis, R.: Vor 100 Jahren brannte in Titisee-Neustadt das Dampfsäge- und Holzwerk Himmelsbach,
760 *Badische Zeitung BZ*, <https://www.badische-zeitung.de/vor-100-jahren-brannte-in-titisee-neustadt-das-dampfsaege-und-holzwerk-himmelsbach--188906523.html>, 2020.

762 Wiederhold, J. G., Christopher J. C., Daniel, K., Infante, I., Bourdon D., and Kretzschmar, R.: Equilibrium
763 Mercury Isotope Fractionation between Dissolved Hg(II) Species and Thiol-Bound Hg, *Environ. Sci.*
764 *Technol.*, 44(11), 4191–4197, DOI:10.1021/es100205t, 2010.

765 Wohlgemuth, L., Osterwalder, S., Joseph, C., Kahmen, A., Hoch, G., Alewell, C., and Jiskra, M.: A bottom-
766 up quantification of foliar mercury uptake fluxes across Europe, *Biogeosci.*, 17(24), 6441-6456, DOI:
767 10.5194/bg-17-6441-2020, 2020.

768 Wright, G., Woodward, C., Peri, L., Weisberg, P. J., and Gustin, M. S.: Application of tree rings
769 [dendrochemistry] for detecting historical trends in air Hg concentrations across multiple scales.
770 *Biogeochem.*, 120(1), 149-162, DOI: 10.1007/s10533-014-9987-9, 2014.

771 Yamakawa, A., Amouroux, D., Tessier, E., Bérail, S., Fettig, I., Barre, J.P., Koschorreck, J., Rüdel, H., and
772 Donard, O.F.: Hg isotopic composition of one-year-old spruce shoots: Application to long-term Hg
773 atmospheric monitoring in Germany, *Chemosphere*, 279, 130631, DOI:
774 10.1016/j.chemosphere.2021.130631, 2021.

775 Yanai, R. D., Yang, Y., Wild, A. D., Smith, K. T., and Driscoll, C. T.: New Approaches to Understand
776 Mercury in Trees: Radial and Longitudinal Patterns of Mercury in Tree Rings and Genetic Control of
777 Mercury in Maple Sap, *Water Air Soil Pollut.*, 231, 1-10, DOI: 10.1007/s11270-020-04601-2, 2020.

778 York, D., Evensen, N. M., Martinez, M. L., and De Basabe Delgado, J.: Unified equations for the slope,
779 intercept, and standard errors of the best straight line, *Am. J. Phys.*, 72(3), 367-375, DOI:
780 10.1119/1.1632486, 2004.

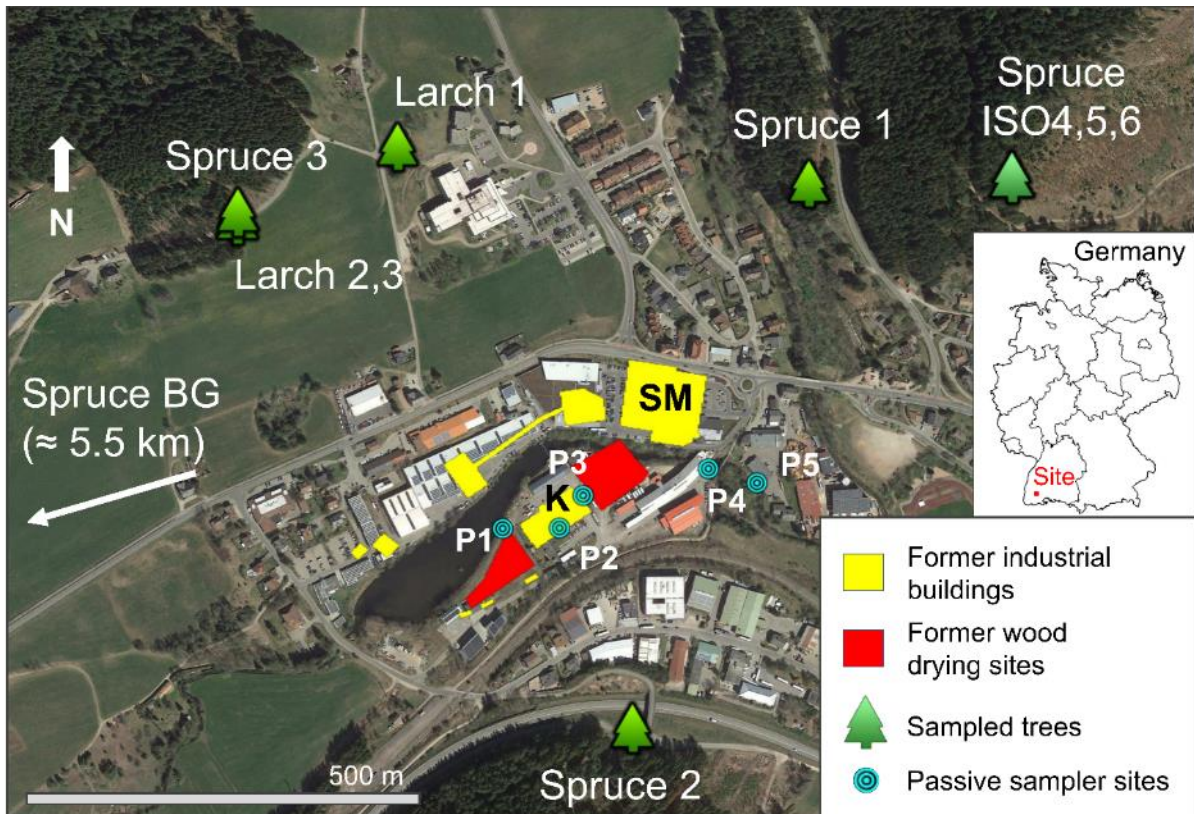
781 Yuan, W., Sommar, J., Lin, C. J., Wang, X., Li, K., Liu, Y., Zhang, H., Lu, Z., Wu, C., and Feng, X.: Stable
782 isotope evidence shows re-emission of elemental mercury vapor occurring after reductive loss from foliage,
783 *Environ. Sci Technol.*, 53(2), 651-660, DOI: 10.1021/acs.est.8b04865, 2018.

784 Zhang, L., Wright, L. P., and Blanchard, P.: A review of current knowledge concerning dry deposition of
785 atmospheric mercury, *Atmos. Environ.*, 43(37), 5853-5864, DOI: 10.1016/j.atmosenv.2009.08.019, 2009.

786 Zheng, W., and Hintelmann, H.: Mercury isotope fractionation during photoreduction in natural water is
787 controlled by its Hg/DOC ratio, *Geochim. Cosmochim. Acta*, 73(22), 6704-6715, DOI:
788 10.1016/j.gca.2009.08.016, 2009.

789 Zhou, J., Wang, Z., Zhang, X., and Gao, Y.: Mercury concentrations and pools in four adjacent coniferous
790 and deciduous upland forests in Beijing, China, *J. Geophys. Res. Biogeosci.*, 122(5), 1260-1274, DOI:
791 10.1002/2017JG003776, 2017.

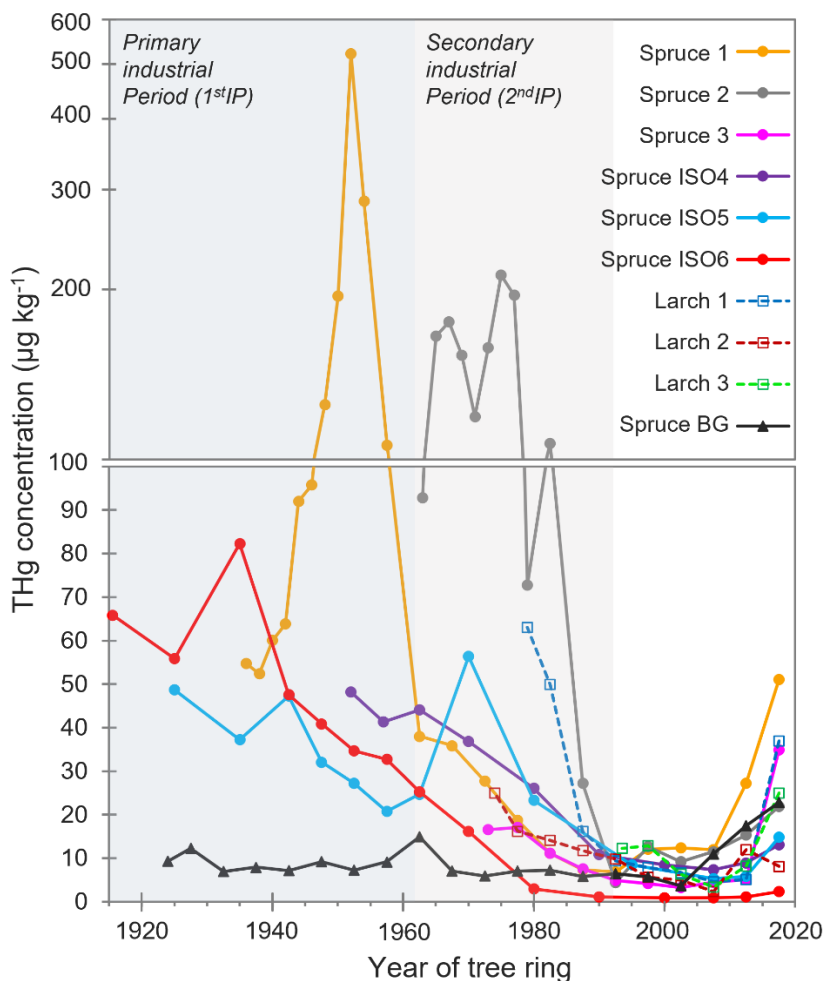
792 Zhou, J., Obrist, D., Dastoor, A., Jiskra, M. and Ryjkov, A.: Vegetation uptake of mercury and impacts on
793 global cycling. *Nature Reviews Earth & Environment*, 2(4), 269-284, DOI: 10.1038/s43017-021-00146-y,
794 2021.



795

796 *Figure 1: Map showing the location of sampled trees, former industrial buildings and wood drying sites*
 797 (*before 1968*), and passive sampler locations (*labelled P1—P5*). The location of Spruce background tree
 798 (*Spruce BG*) is \approx 5.5 kilometres west southwest of the study site (*direction indicated on map*). SM – *Former*
 799 *sawmill*; K – *former kyanisation hall/wood treatment area*. The three Spruce ISO trees are from the
 800 *deforested stand in the northwest of Fig. 1; exact location of each of these trees within this stand is unknown*
 801 (*trees felled by forest workers*). ©Google Earth 2019.

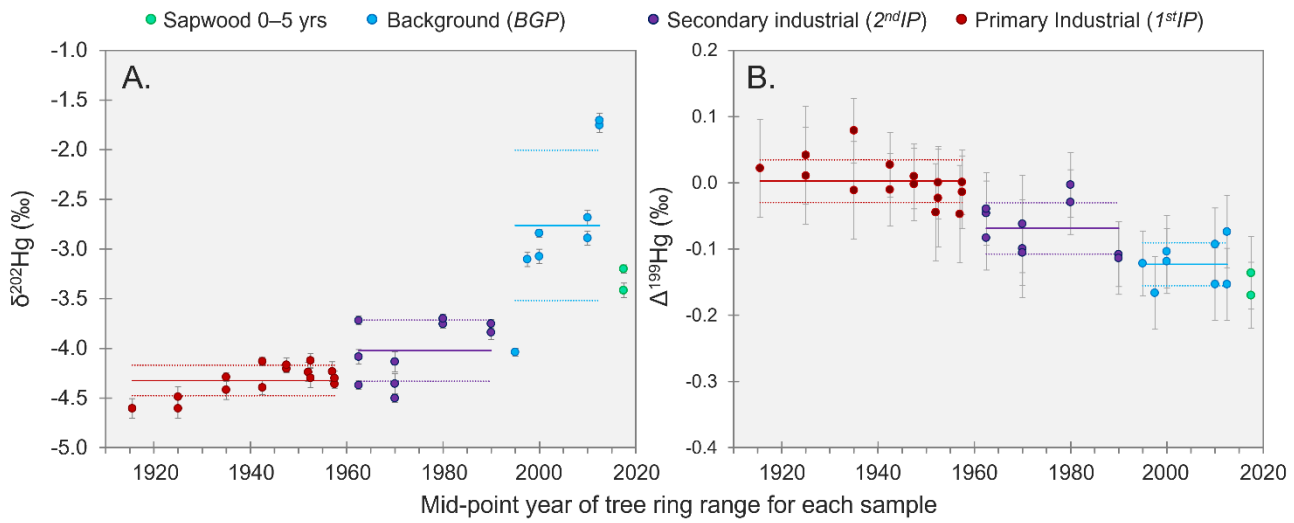
802



803

804 **Figure 2:** THg concentrations in tree rings dated by year. Years of tree rings correspond to the middle
 805 point of samples of combined adjacent rings (i.e., 0—5 year = 2.5 years). Y-axis is split at $100 \mu\text{g}\cdot\text{kg}^{-1}$
 806 changing from normal- to log-scale due to the very high concentrations measured in Spruce 2.
 807 1stIP (before 1962) and 2ndIP (1962—1992) are highlighted.

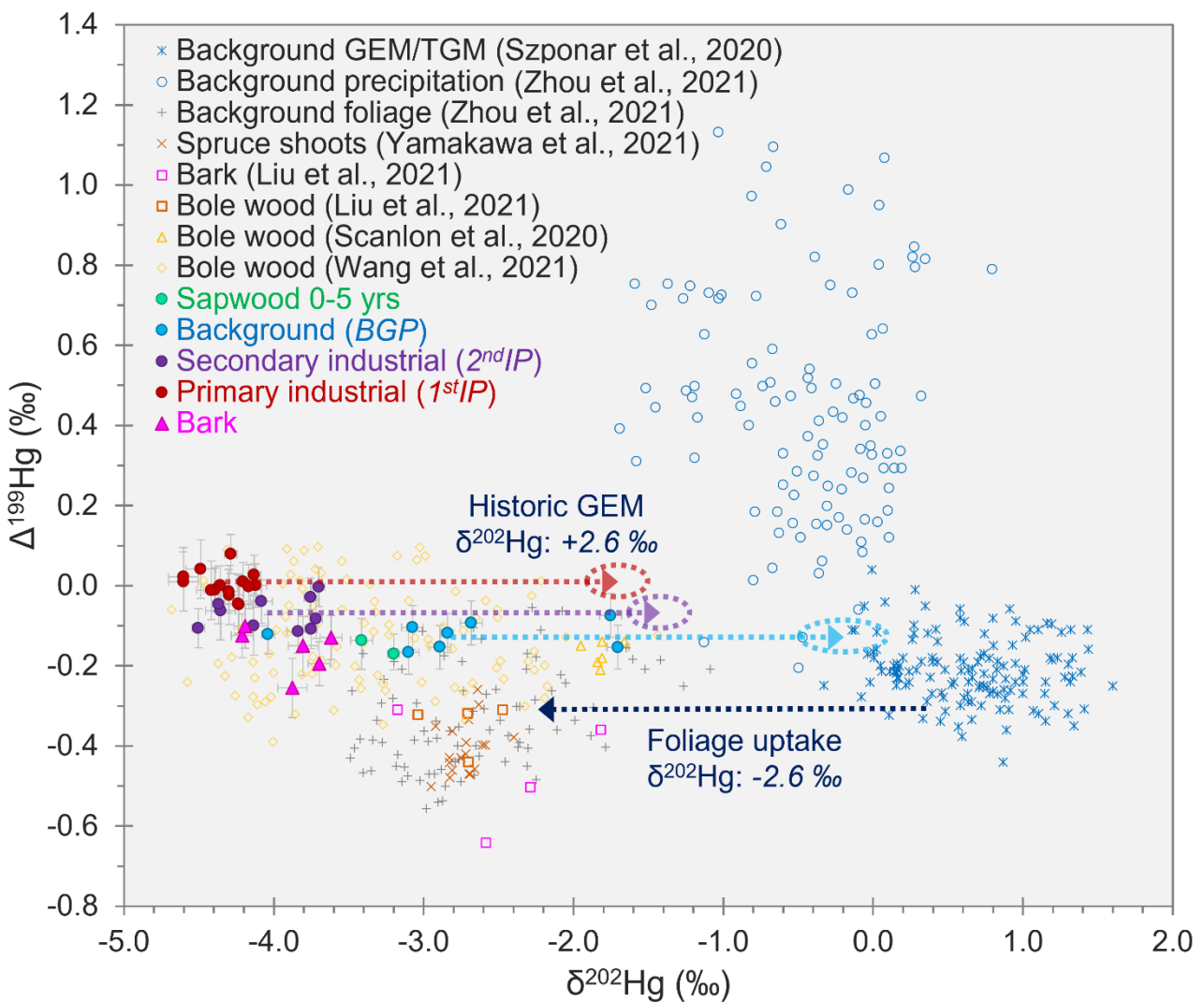
808



809

810 **Figure 3:** $\delta^{202}\text{Hg}$ (Panel A) and $\Delta^{199}\text{Hg}$ (Panel B) in tree rings dated by year for samples from Spruce
 811 ISO4—6 trees. Solid and dotted lines for each period represent the mean and standard deviation,
 812 respectively. Data displayed are the composite of all three trees (figures for individual trees are shown in
 813 Section S6). Data for THg plotted against MDF and THg against MIF are shown in Section S7. Error bars
 814 for individual datapoints represent session 2SD for secondary standard “ETH Fluka”.

815



816

817 **Figure 4:** Relationships between $\Delta^{199}\text{Hg}$ and $\delta^{202}\text{Hg}$ for tree rings samples from Spruce ISO4—6 trees
 818 analysed for Hg stable isotopes (data with solid markers). Figure includes the $\Delta^{199}\text{Hg}$ and $\delta^{202}\text{Hg}$ values for
 819 tree samples (bole wood, bark, foliage, and shoots) from other studies. Additionally, background TGM/GEM
 820 data were included to show the $\approx -2.6\text{‰}$ MDF associated with stomatal uptake of GEM (dark blue dotted
 821 line), and background precipitation samples were included to demonstrate that there was little influence
 822 from precipitation on found Hg in within trees. The red, purple, and light-blue dotted lines indicate the
 823 predicted GEM values in air at the site during the 1stIP, 2ndIP, and BGP, respectively, based off the mean
 824 measured $\delta^{202}\text{Hg}$ values in tree rings for these respective periods (MIF was assumed to be zero for stomatal
 825 uptake in these calculations).

826